World Research Journal of Applied Physics
ISSN: 0976-7673 & E-ISSN: 0976-7681, Volume 4, Issue 1, 2013, pp.-54-58.
Available online at http://www.bioinfopublication.org/jouarchive.php?opt=&jouid=BPJ0000280

STACKING FAULTS AND MICRO STRUCTURAL PARAMETERS IN NANO MAGNESIUM OXIDE (MgO) PARTICLES USING WHOLE PATTERN FITTING TECHNIQUE

MAHESH S.S.[1]*, NANDAPRAKASH M.B.[2] AND SOMASHEKAR R.[2]

[1]Department of Physics, Acharya Institute of Technology, Bangalore- 560 090, Karnataka, India.
[2]Department of Studies in Physics, University of Mysore, Manasagangotri, Mysore- 570 006, Karnataka, India.
*Corresponding Author: Email- maheshphysics1976@gmail.com

Received: September 28, 2013; Accepted: October 21, 2013

Abstract- Nano-composites of Magnesium Oxide nanoparticles are synthesized by solution combustion method employing Sucrose as fuels with corresponding metal nitrates. The synthesized nano particles by solution combustion method were subjected to XRD and SEM analysis for the characterization process for estimating the size of crystalline particle and figure out the morphology. The as-prepared powders are all nano-sized (180-260 nm) and the same is confirmed by broadening of the X-ray diffraction peaks and Scanning electron microscopy. XRD results show that Crystallite area increases with increasing temperature. The crystallite size (<N>), lattice strain (g in %), stacking faults (α^d) and twin faults (β) determined by whole powder pattern fitting technique, developed by us. We have studied the microcrystalline parameters from XRD. Activation energy has been computed for these systems.

Keywords- Stacking faults, Twin faults, crystallite area, WAXS, Solution combustion method

Citation: Mahesh S.S., Nandaprakash M.B. and Somashekar R. (2013) Stacking Faults and Micro Structural Parameters in Nano Magnesium Oxide (MgO) Particles using Whole Pattern Fitting Technique. World Research Journal of Applied Physics, ISSN: 0976-7673 & E-ISSN: 0976-7681, Volume 4, Issue 1, pp.-54-58.

Introduction

Magnesium oxide (MgO), or *magnesia*, is a white hygroscopic solid mineral that occurs naturally as Pericles and is a source of magnesium. It has an empirical formula of MgO and consists of a lattice of Mg^{2+} ions and O^{2-} ions held together by ionic bonds. Magnesium hydroxide forms in the presence of water ($MgO + H_2O \rightarrow Mg(OH)_2$), but it can be reversed by heating it to separate moisture. Magnesium oxide was historically known as magnesia alba (literally, the white mineral from Magnesia), to differentiate it from *magnesia negra*, a black mineral containing what is now known as manganese. Magnesium oxide is produced by the calcinations of magnesium carbonate or magnesium hydroxide or by the treatment of magnesium chloride with lime followed by heat.

Nanoscale MgO powders have attracted great attention owing to its applications in many industrials areas, such as a candidate material for translucent ceramics [1], catalyst, catalyst carriers and absorbent for many pollutants [2]. Thus, many extensive studies have been carried out to synthesize nanoscale MgO powders using various novel wet chemical methods, e.g. sol-gel synthesis, followed by supercritical drying [3]. However, these techniques usually include many sophisticated processes and consume much longer time. Moreover, they have not received much commercial attention due to lacking of reproducibility, reliability and cost effectiveness [4-6]. At the same time, solution combustion synthesis may provide an answer to some of the above-mentioned problems. Therefore, extensive studies have been conducted to investigate solution combustion synthesis and characteristics of MgO powders, the group of Granados-Correa [7] synthesized MgO powders via a solution combustion process using urea as fuel. In addition, Rao & Sunandana [8] also fabricated MgO nanoparticles using the solution combustion technique with urea as fuel. Moreover, Mortazavi, et al [9]produced high activity MgO nanoparticles with large surface areas via a microwave-induced combustion process using polyethylene glycol and sorbitol as fuel.

In this work, MgO nanoparticles were synthesized via a microwave-induced combustion process using sucrose as fuel. In addition,. The crystallite size (<N>), lattice strain (g in %), stacking faults (α^d) and twin faults (β) as-prepared powders were also determined by whole powder pattern fitting technique, developed by us. The synthesized nano particles by solution combustion method were subjected to XRD and SEM analysis for the characterization process for estimating the size of crystalline particle and figure out the morphology.

Material and Methods

Synthesis of Magnesium oxide Nano Particles by Solution Combustion Method

The Magnesium oxide nanoparticles are produced by dissolving 2 g of Magnesium nitrate with 0.6 g of Sucrose (Sugar) in 20 ml of distilled water. The mixture was taken in borosilicate petri dish and it was heated to 300°C and 500°C in a Maffle Furnace separately for about 20 to 30 minutes to obtain Magnesium oxide nanoparticles.

2 gm of Magnesium Nitrate + 0.6 gm of Sucrose + 20 ml of distilled water	500°C →	Magnesium Oxide nanoparticles
2 gm of Magnesium Nitrate + 0.6 gm of Sucrose + 20 ml of distilled water	300°C →	Magnesium Oxide nanoparticles

Experimental Procedure

Scanning Electron Microscopy (SEM)

The scanning electron microscope (SEM) uses a focused beam of high-energy electrons to generate a variety of signals at the surface of solid specimens. The signals that derive from electron-sample interactions reveal information about the sample including external morphology (texture), chemical composition, and crystalline structure and orientation of materials making up the sample. In most applications, data are collected over a selected area of the surface of the sample, and a 2-dimensional image is generated that displays spatial variations in these properties. Areas ranging from approximately 1 cm to 5 microns in width can be imaged in a scanning mode using conventional SEM techniques (magnification ranging from 20X to approximately 30,000X, spatial resolution of 50 to 100 nm). The SEM is also capable of performing analyses of selected point locations on the sample; this approach is especially useful in qualitatively or semi-quantitatively determining chemical compositions, crystalline structure, and crystal orientations. The design and function of the SEM is very similar to the EPMA and considerable overlap in capabilities exists between the two instruments.

The SEM photographs helped to find the morphology of nanoparticles and the average particle size can be calculated by plotting the diagonal line on the image. The point of intersection is counted and using the following formula we can calculate the average particle size.

Average particle size = D/M*N

where,

D = Diameter of the line plotted on the image.

M = Magnification of the image.

N = Number of intercepts.

[Fig-1] shows the SEM photograph of Magnesium oxide with Sucrose at 500°C. The Magnesium oxide nanoparticles are spherical in structure and they have more surface area. These Magnesium oxide nanoparticles which are synthesized with Sucrose at 500°C are more porous in nature.

Average particle size = $6.1*10^{-2}/47*500$ = 260 nm

The average particle size of Magnesium oxide nanoparticles which are synthesized with Sucrose at 500°C is 260 nm.

[Fig-2] shows the SEM photograph of Magnesium oxide with Sucrose at 300°C. The Magnesium oxide nanoparticles are spherical in structure and they have more surface area. These Magnesium oxide nanoparticles which are synthesized with Sucrose at 300°C are more porous in nature.

Average particle size = $6.2*10^{-2}/43*8000$ = 180nm

The average particle size of Magnesium oxide nanoparticles which are synthesized with Sucrose at 300°C is 180 nm. There is no much difference between the Magnesium oxide nanoparticles which are synthesized with Sucrose at 300°C and 500°C.

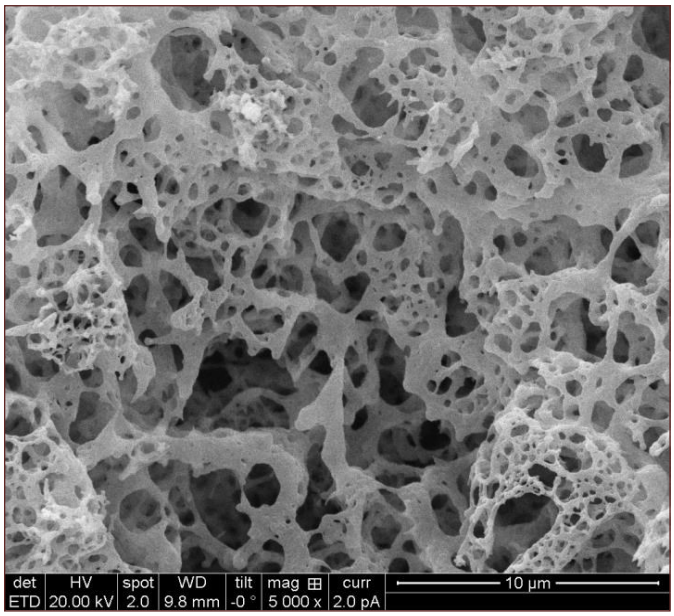

Fig. 1- SEM photograph of Magnesium oxide with sucrose at 500°C

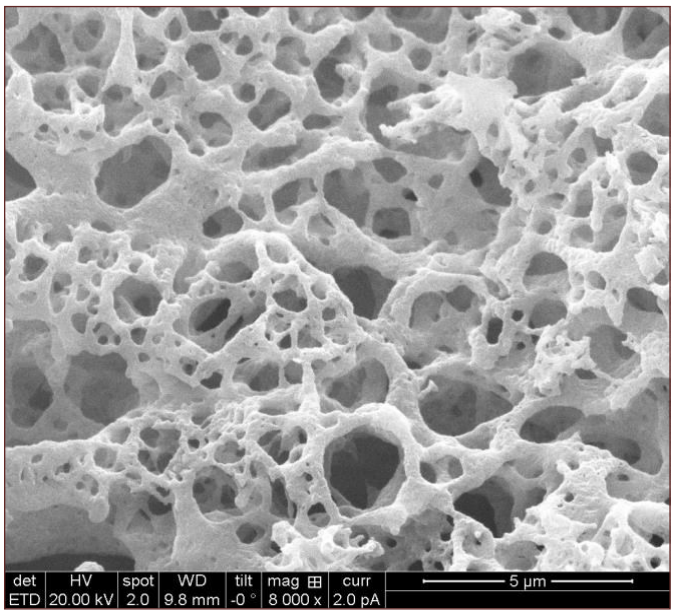

Fig. 2- SEM photograph of Magnesium oxide with sucrose at 300°C

The X-ray Diffraction Pattern

X-ray diffraction pattern of MgO samples were recorded on Rigaku Miniflex II Diffractometer with Ni filtered CuK_α radiation of wavelength 1.542 Å, and a graphite monochromator. The scattered beam from the sample was focused on to a detector. The specifications used for the recording were 30 kV and 15 mA. The MgO sample was scanned in the 2θ range of 6° to 60° with a scanning step of 0.02°. The X-ray scattering measurements were performed at the WAXS/SAXS beam line of the LNLS (Laboratorio Nacional de Luz Sincroton-Campinas, Brazil), by using monochromatic beam of wavelength 1.7433 Å. The scattering intensity was registered using a one dimensional position-sensitive gas detector for a sample-detector distance of 1641.5 mm. The scan range (2θ) was 10° to 50°. WAXS curves were obtained from the WAXS images by band integration tool supplied by X-ray 1.0 software, produced by Universite Mons Hainaut.

Theory

X-ray Diffraction Data Analysis

The contribution of crystallite size, lattice strain and stacking faults to a Bragg reflection profile can be written as [10],

$$I_{hkl}(s_{hkl}) = \int_{-\infty}^{\infty} T^{IP}(nd) e^{[2\pi i\zeta(nd)]} e^{[2\pi i\phi(nd)]} e^{[2\pi i n d s_{hkl}]} d(nd) \quad (1)$$

where $I_{hkl}(s_{hkl})$ is the intensity of a profile in the direction joining the origin to the center of the reflection, T^{IP} is the Fourier transform of instrument profile, $e^{[2\pi i\zeta(nd)]}$ is the average phase factor due to lattice distortion(ζ) and $e^{[2\pi i\varphi(nd)]}$ is due to crystallite size / stacking faults(φ). L = nd (with d=d_{hkl}) is the column length. [Eq-1] can be written in the form of Fourier series as,

$$I_{hkl}(s_{hkl}) = \sum_{n=-\infty}^{\infty} A_{hkl}(n) \cos\{2\Pi n d_{hkl}(s-s_0)\} \quad (2)$$

where $A_{hkl}(n)$ are corrected Fourier coefficients with Fourier coefficients of instrumental profile function $T^{IP}(nd)$, s is sinq/l and s_0 is the value of s at the peak of the reflection. Here afterwards, we refer to crystallite size in terms of the average number of unit cells counted in a direction perpendicular to the Bragg plane (hkl) with a notation <N>, and the crystallite size in Å is given by D_{hkl} = <N>d_{hkl} (d_{hkl} is the perpendicular spacing of the (hkl) planes from their origin). These Fourier coefficients $A_{hkl}(n)$ are functions of the size of the crystallite, the disorder of the lattice and stacking faults coefficients, i.e.

$$A_{hkl}(n) = A^{s}{}_{hkl}(n).A^{d}{}_{hkl}(n).A^{F}{}_{hkl}(n) \quad (3)$$

Fourier analysis of a Bragg reflection profile must always be performed [11] over the complete cycle of the fundamental form d (s-s_o) = -1/2 to +1/2, which is rarely possible experimentally. We do this analysis with the available truncated range by introducing truncated correction [12]. For a paracrystalline material, with Gaussian strain distribution, $A^{d}{}_{hkl}(n)$ turns out to be[11,13-14],

$$A^{d}{}_{hkl}(n) = \exp(-2\Pi^2 n^2 m g^2) \quad (4)$$

where m is the order of the reflection and g = (Δd/d) is the lattice strain. Normally one also defines mean square strain $\langle\varepsilon^2\rangle$ that is given by g^2/n. This mean square strain is dependent on n (or column length L = nd), where as g is not. With exponential distribution function for column length, we have,

$$A^{S}_{hkl}(n) = \begin{cases} A(0)\left(1 - n/\langle N\rangle\right), & ;if\ n < p \\ A(0)\left\{\exp\left[-\alpha(n-p)\right]\right\}/(\alpha N) & ;if\ n \geq p \end{cases} \quad (5)$$

In [Eq-5] α = 1/(N-p), refers to the width of the distribution and p is the smallest number of unit cells in a column.

Warren [11] has given an integral analysis for deformation faults and twin faults in various crystal systems. According to this paper, the shift, broadening and asymmetry of the profile are proportional to these fault densities. The sequence of stacking layers is usually denoted by A, B and C. The unfaulted sequence is ABCABC or CBACBA. A stacking fault can be represented by ABCBCABC. A twin fault sequence is ABCABCBACBA. The chance of finding a stacking fault between any two adjacent layers causing a Bragg reflection and is denoted by α^d. Normally α^d is expressed in percentage and the average number of Bragg planes between stacking faults is given by 1/ α^d. The twin fault probability β is defined as the chance of finding a twin fault between any two adjacent (hkl) layers and the average number of (hkl) layers between twin faults is 1/β. With these aspects, Veltrop [15] has obtained an equation for Fourier coefficients $A^{F}{}_{hkl}(n)$ in terms of the deformation faults (α^d) and twin faults (β) probabilities as

$$A^{F}_{hkl}(n) = [1 - 3\alpha^d - 2\beta + 3(\alpha^d)^2]^{|(1/2)nd_{hkl}s(L_0/h_0^2)\sigma_{L_0}|} \quad (6)$$

where α^d and β are, respectively the deformation and twin fault probabilities, L_0=h+k+l, h^2_0=h^2+k^2+l^2 and σ_{L_0} is the volume of crystallite with specified L_0. We have assumed σ_{L_0} to be positive for all reflections (for L_0=3N+1 and N = 0, ±1, ±2, . . .) studied here. The whole powder pattern of samples were simulated using individual Bragg reflections represented by the above equations using

$$I(s) = \sum_{hkl}(\omega_{hkl} I_{hkl} - BG) \quad (7)$$

where ω_{hkl} are the appropriate weight functions for the (hkl) Bragg reflection. Here s takes the whole range (2θ ≈ 6° to 60°) of X-ray diffraction recording of the sample. BG is an error parameter introduced to correct the background estimations.

Results and Discussion

In the first step, the micro structural parameters were refined for individual profiles of X-ray recordings in each of the sample and the computed values of crystallite size <N>, lattice strain (g in %), stacking fault probability and twin fault probability are given in [Table-1] and [Table-2] for Magnesium Oxide Nano Particles using exponential distribution function at 300°C and 500°C. We observe that the lattice strain in both is 0.1% and average crystallite area increases in Magnesium Oxide Nano Particles with sucrose as temperature increases from 225.6 Å^2 to 368.9 Å^2.

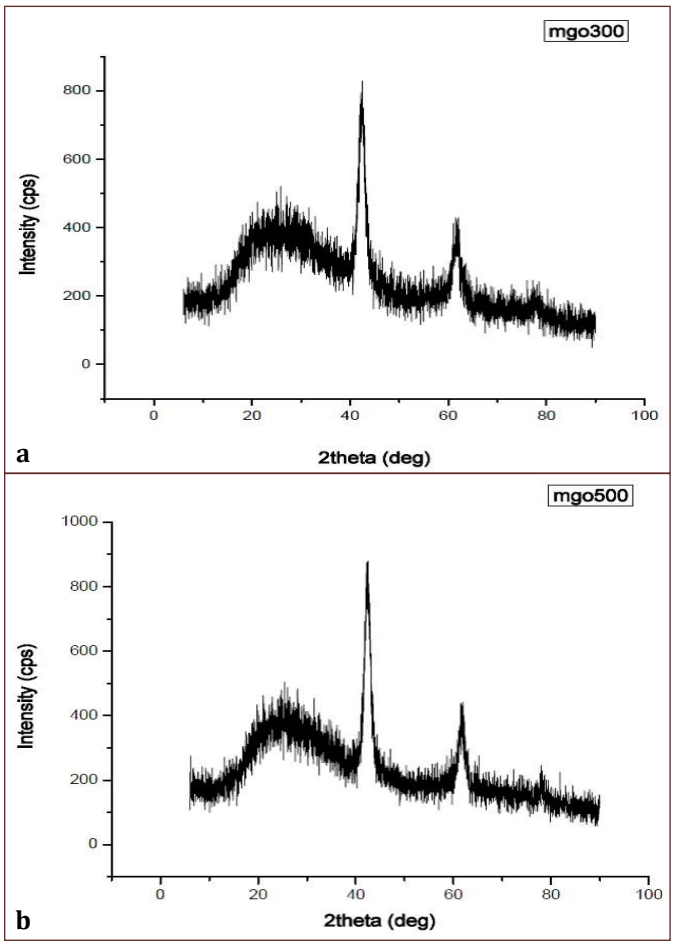

Fig. 3- X-ray diffraction patterns obtained MgO 300 (3a) and MgO 500 (3b).

[Fig-3] shows X-ray diffraction patterns obtained MgO 300 and MgO 500. [Fig-4] shows simulated and experimental profiles for MgO Nano particles with sucrose at 300°C and 500°C obtained with exponential column length distribution.

The standard deviations in all the cases for the micro structural parameters are given in [Table-1] and [Table-2] as Δ. This Δ represents the statistical percentage of deviation of the parameters. The agreement between simulated and experimental intensity of the individual profiles in each of the samples are less than 10% of the mean value. With these parameters given in [Table-1] and [Table-2] as an input, we have further refined these parameters against the whole pattern (2θ ≈ 6° to 60°) recorded from the samples by taking summation which extends over the whole pattern [Eq-7]. We have observed small but significant changes in these parameters with the set convergence of 1%. These changes are also given in [Table-1] and [Table-2]. The goodness of the fit between simulated and experimental profiles for the samples were given in [Fig-4].

The observed variation in the micro structural parameters given in [Table-1] and [Table-2] is due to a two-fold refinement. First we have carried out the line profile analysis of the extracted profiles from overlapping regions, which is a standard procedure to compute the micro structural parameters. Secondly, the range of overlapping regions determines the extent of broadening of the reflections. In fact, the broadening may decrease if the reflections are closer together and hence results in an increase in the crystallite size values. A closer look at the results in [Table-1] and [Table-2] and also the whole pattern indicates such a problem. It is worth noting that none of other parameters, such as lattice strain and stacking fault probability, varied much during the refinement against the whole pattern data of the samples.

Table 1- Micro structural parameters and stacking faults for MgO 300 using exponential distribution function

2θ	N	D (Å)	D (Å)	g (%)	α	α^d	β	delta	Crystallite area (Å²)
22.01	2.54	4.035	10.25	0.1	8.85	1.29E-04	5.19E-05		
30.27	1.87	2.95	5.517	0.1	8.062	1.89E-07	4.86E-07		
42.4	19.2	2.13	40.89	0.1	5.756	2.84E-05	9.89E-07		
44.72	14.2	2.024	28.74	0.1	0.848	2.87E-06	2.52E-05	0.1887	225.6
50.64	3.7	1.801	6.664	0.1	3.759	3.33E-05	1.98E-04		
61.66	26.9	1.503	40.43	0.1	0.403	9.39E-05	4.40E-07		
65.78	4.08	1.418	5.785	0.1	9.697	4.41E-05	7.46E-08		

Table 2- Micro structural parameters and stacking faults for MgO 500 using exponential distribution function

2θ	N	D (Å)	D (Å)	g (%)	α	α^d	β	delta	Crystallite area (Å²)
24.08	2.05	3.692	7.569	0	7.067	4.89E-06	1.04E-05		
30.63	2.2	2.916	6.415	0	4.995	7.70E-07	3.81E-07		
42.4	27	2.13	57.51	0	4.325	7.32E-06	2.03E-05		
44.96	7.3	2.014	14.7	0	1.339	1.69E-05	9.32E-05	0.1402	368.9
52.06	9.7	1.755	17.02	0	0.933	5.78E-08	6.36E-07		
61.81	27	1.499	40.47	0.1	2.765	1.93E-05	9.11E-06		
78.18	6.7	1.222	8.187	0	0.922	5.95E-07	2.31E-07		

To check the reliability of the computed deformation and twin faults, we have used a simple approximate method suggested by Warren [11] and the expression for the twin fault is given by,

$$(2\theta^{\circ}_{CG} - 2\theta^{\circ}_{PM})_{hkl} = -14.6 X_{hkl} \tan\theta \; x \; \beta \qquad (8)$$

where $2\theta^{\circ}_{CG}$ is the center of gravity of the Bragg reflection profile and $2\theta^{\circ}_{PM}$ is the peak maxima, β is the twin fault and X_{hkl} is the constant value, which we have taken to be 0.23. For all the samples we have computed the average twin fault probabilities are comparable to the values obtained by incorporating an appropriate expression in the Fourier coefficients. From this we would like to emphasize that these values are reliable and do represent the twin faults present in the sample in a direction perpendicular to the axis of sample. In fact, 1/β represents the number of layers between two consecutive twin fault layers. We have also approximately estimated the deformation fault probability value α^d by making use of the following expression given by Warren [11],

$$\frac{1}{< D_S >} = \frac{1}{< D >} + [(1.5\alpha^d + \beta)/d_{hkl}]\,[\sum_b |L_0|/(u+b)h_0] \qquad (9)$$

where $h_0=(h^2+k^2+l^2)^{1/2}$, u is the un broadened component, b is the broadened component and $L_0=3N+1$ reflections. A comparison with the deformation fault probability values obtained by Fourier coefficient method [Table-1] and [Table-2] indicates that the values are low, because there are too many layers between two successive deformation fault layers. This is due to the fact that there are pockets of crystalline like order in a matrix of amorphous regions. It is well known that the Fourier method gives a reliable set of micro structural parameters and we have shown that in addition to these values, one can also compute reliable fault probabilities.

[Fig-5](a) shows the variation of stacking faults with crystallite size for MgO 300 K and [Fig-5](b) Variation of twin faults with crystallite size for MgO 500 K

A graphical plot of the crystallite shape ellipse was obtained by taking the crystal size value corresponding to 2θ ≈ 22.01° along the X-axis and the other parameter corresponding to 2θ ≈ 65.78° along the Y-axis for MgO Nano particles with Sucrose at 300°C and 2θ ≈ 24.08° along the X-axis and the other parameter corresponding to 2θ ≈ 78.18° along the Y-axis for MgO Nano particles with sucrose at 500°C shown in [Fig-6].

These crystallite shape ellipse for the different samples the strength of the samples are normally proportional to crystalline area which is equal to ellipse area determined by micro structural parameters. It is evident that the crystallite shape ellipse areas in MgO Nano particles with Sucorse increases with temperature.We have calculated the probability of finding a hexagonal or cubic environment in the

stacking arrangement, which are the parameters used in the early works of Jagodzinski [15,16] and these values are given in the [Table-1] and [Table-2].

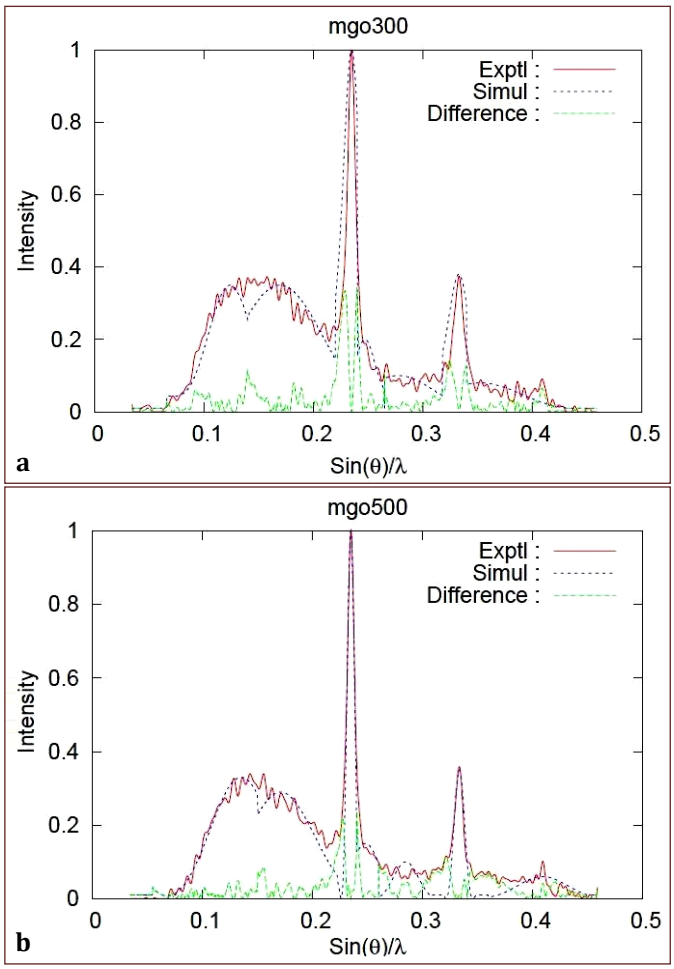

Fig. 4- Simulated and experimental profiles for MgO 300 (4a) and MgO 500 (4b) obtained with exponential column length distribution

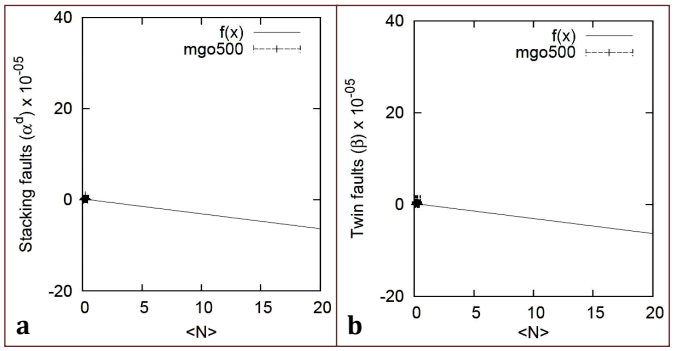

Fig. 5- Variation of stacking faults with crystallite size for MgO 30 (5a); Variation of twin faults with crystallite size for MgO 500 (5b)

Conclusion

Whole X - ray pattern fitting procedure developed by us has been used to compute micro crystalline parameters. Electron scanning micrograph study of MgO with sucrose gives a value of the particle size in conformity with the X - ray results. The average particle size of Magnesium oxide nanoparticles which are synthesized with Sucrose at 500°C is 260nm. The average particle size of Magnesium oxide nanoparticles which are synthesized with Sucrose at 300°C is 180 nm. The important aspect of this investigation is that MgO nano particles have more Crystalline area than other samples studied here.

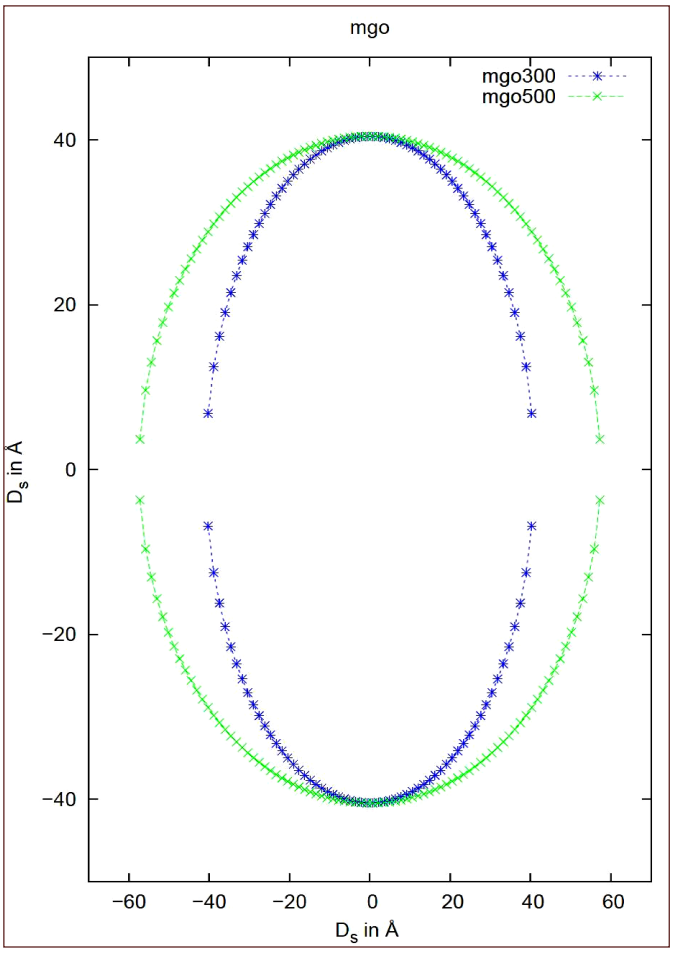

Fig. 6- Variation of crystallite shape ellipsoid for MgO 300 and MgO 500

Conflict of Interest: None declared.

References

[1] Misawa T., Moriyoshi Y., Yajima Y., Takenouchi S., Ikegami T. (1999) *J. Ceram. Soc. Jpn.*, 107(4), 343-348.

[2] Chen L.M., Sun X.M., Liu Y.N., Li Y.D. (2004) *Appl. Catal. A: Gen.*, 265, 123-128.

[3] Bedilo A.F., Sigel M.J., Koper O.B., Melgunov M.S.,Klabunde K.J. (2002) *J. Mater. Chem.*, 12, 3599-3604.

[4] Aruna S.T. (2008) *Current Opinion in Solid State and Materials Science*, 12, 44-50.

[5] Patil K.C., Aruna S.T., Mimani T. (2002) *Current Opinion in Solid State and Materials Science*, 6, 507-512.

[6] Ianos R., Lazau I. (2009) *Mater. Chem. Phys.*, 115, 645-648.

[7] Granados-Correa F., Bonifacio-Martínez J., Lara V.H., Bosch P., Bulbulian S. (2008) *Applied Surface Science*, 254(15), 4688-4694.

[8] Venkateswara Rao K., Sunandana C.S. (2008) *J. Mater. Sci.*, 43, 146-154.

[9] Esmaeili E., Khodadadi A., Mortazavi Y. (2009) *Journal of the European Ceramic Society*, 29(6), 1061-1068.

[10]Scardi P. and Leoni M. (2002) *Acta. Cryst*., A58, 190-200.

[11]Warren B.E. (1969) *X-ray Diffraction,* Courier Dover Publications.

[12]Somashekar R., Hall I.H. and Carr P.D. (1989) *J. Appl. Cryst.,* 22, 363-371.

[13]Warren B.E. (1959) *Prog. Met. Phys*., 8, 147-202.

[14]Warren B.E., Averbach B.L. (1950) *Journal of Applied Physics*, 21(6), 595-599.

[15]Veltrop L., Delhez R., De Keijser Th.H., Mittemeijer E.J. and Reefman D. (2000) *J. Appl. Cryst.*, 33, 296-306.

[16]Jagodzinski H. (1949) *Acta Cryst.*, 2, 201-207.